Int. J. Econ. Environ. Geol. Vol. 16 (3) 55-65, 2025
Journal home page: www.econ-environ-geol.org

Open Access
ISSN (Online) 2223-957X

Geological and Geochemical Characteristics of Sharote Copper Deposit Kohistan Island Arc, Gilgit Baltistan

Masroor Alam[1*], Naeem Ul Khaliq Jan[1], Atif Hussain[2], Muhammad Azam[1]

[1]Department of Geology and Mountain Hazards Karakoram International University Gilgit, Pakistan
[2]Department of Geographic Information System, School of Computing and Emerging Technologies, Karakoram International University Gilgit, Pakistan

Corresponding author E-mail: masroor.alam@kiu.edu.pk

Received: *2 September, 2025* ***Accepted:*** *28 September, 2025*

Abstract: This study presents first report on hydrothermal polymetallic ore deposit in the Sharote Valley some 29 km North-West from Gilgit city in the northern Kohistan Island Arc Gilgit Baltistan. The deposit is formed of extending sulphide veins. The minerals in associated rocks are identified as quartz, biotite, muscovite, epidote, plagioclase and hornblende amphibole with accessory minerals chlorite, sericite with opaques. The XRF analysis of investigated rocks shows that the major oxides are Na_2O (6.10-6.70 wt. %), CaO (2.73-5.49 wt. %), SiO_2 (66.69-68.10 wt. %), Fe_2O_3 (1.0-3.92 wt. %) Al_2O_3 (4.55-8.59 wt. %), and K_2O (2.1-2.28 wt. %), which indicate that the associated rock is quartz monzonite which is more Calc-alkaline and less tholeiitic based on AFM diagram. Based on the analysis of ore samples using Atomic Absorption Spectroscopy, the trace elements Cr, Zn, Co, Pb, Fe, Mn, Ni, Au, and Ag are investigated. The concentration (Wt.%) of Au, Ag, Cu, Cr, Pb, Ni, Co, Zn are 0.04-0.296, 4.2-42.55, 851.25-20025, 2.25-12.9, 2.1-1105, 0.1-28.25, 78.75-252.5 and 17.45-280.45. Cu shows positive trends with Co, Cr, Zn, Ag and Pb. These geochemical signatures, petrographic results and field observations show that sulphide veins dominated by chalcopyrite and bornite, accompanied by secondary azurite and malachite, and hosted within quartz monzogranite are best interpreted as products of a magmatic-hydrothermal system linked to the emplacement and crystallization of the granitic intrusion. As magma evolved, metals such as Cu, Au, Pb, and Fe, along with volatiles (H_2O, S, Cl, and CO_2), became progressively concentrated in the residual melt. Upon reaching fluid saturation, metal-bearing hydrothermal fluids were exsolved from the crystallizing quartz monzogranite. These fluids, enriched in Cu–Au complexes, constituted the primary source of the sulphide mineralization.

Keywords: Sharote Valley polymetallic deposit, geochemistry; petrography, Kohistan Island Arc, Gilgit, Pakistan.

Introduction

The characterization of the ore is a very essential step performed before any processing, thereby determining the quantity, shape, grade or quality, and geochemical characteristics to allow the appropriate application of technical and economic parameters to support the production plan and evaluate the economics of the deposit feasibility (Kiptarus et al., 2015). Ore deposits are formed by geologic or tectonic processes ranging from magmatic crystallization to weathering (Robb, 2005).

The igneous rocks host large number of different ore deposits including vesicular filling deposits, extrusive rocks related massive sulfide deposits and widespread mineralization of base metals (copper, ten, silver, gold). They also include intrusions possessing stratiform deposits such as chromite, magnetite and ilmenite, may extend over many kilometers, as in the Bushveld Complex of South Africa (Evans, 2009).

Hydrothermal events associated with shear zones, fold limbs, regional decollements, and interfaces areas enhanced ore deposits in igneous rocks (Evans, 2009).

Hydrothermal vein minerals in igneous rocks have solidified or have been changed by hot water flowing across it. Hydrothermal deposits can be found in extension-driven subsidence basins from any geological epoch (Kyser, 2007).

Hydrothermal networks are generally accompanied by the emplacement of fragmented, hydrous magma chambers at shallower depths. At all scales of observation, fractures and interconnected open spaces of the shear zone accept metallic minerals bearing solution and create metallic ore in the form of veins (Bauer, et al., 2000).

This study mainly focused on hydrothermal mineralization vein polymetallic ore deposit (sulphides and oxides mix and as well rich percentage

of iron) in Sharote valley North to West in 29 km distance from Gilgit with an altitude of 5416 ft. from sea level. The mineralized vein is mainly exposed between upper contact Meta sedimentary rock and lower contact meta-volcanic rocks. A rich mineralized iron vein with visible oxide and sulphide content travelling horizontally in south to north direction with granodiorite contact fault.

The vein visibly measures 1.5 meters wide at surface running visually for 500 meters in a sub-surface and outcrop pattern at -5-degree decline angle. The high-grade vein seems to visually dip and travel further in the mountain face. The vein is primarily composed of malachite, chalcopyrite and azurite, and some tinges of bornite copper ore with a good amount of iron ore (Fe hematite), slight Lead (Pb) and little manganese (Mn) and hints of cobalt as well.

Furthermore, this study also aims to find copper, iron, gold and associated metals mineralization (sulphides and oxides and as well Au) in the Sharote Valley. The deposit was not previously studied, and the metal contents and their precipitation mechanism are unknown. In this contribution, we adopted multiparametric techniques to evaluate the geological and geochemical features to evaluate gold and associated metal contents and their precipitation mechanisms.

Regional and Deposit Geology

Gilgit Baltistan is divided into three tectonic-zones which are Indo Pakistan plate, Kohistan Island Arc and Karakoram plate, from south-north. The Indian and Karakoram plates are wedged by the K.I.A (Kohistan-Island-Arc), which has two major thrust faults. It is detached by the Main Mantle Thrust to the south from the Indian Plate and separated by the Main Karakorum Thrust to the north from the Karakoram Plate (Burg et al., 1998).

The Kohistan Island Arc (KIA) is an intra-oceanic arc that runs across the Karakoram Himalaya terrain and is the result of a massive tectonic collision between the Indo-Pakistan and Eurasian (Asian) plates, as well as the neo-Tethys Ocean closing (Treloar et al., 1996). The Kohistan Island Arc (KIA) is a Cretaceous-era Island arc. In the Indus Suture Zone (ISZ), the KIA has a southern contact with the Indo-Pakistan plate and a northern contact with the Eurasian Plate along the Northern Suture Zone (NSZ).

The existence of transitional zones (Suture zones) on both the southern and northern margins, as well as the evolution of KIA, is widely accepted and well known. Kohistan Island Arc is comprised of volcanic and plutonic rocks with some meta sediments such as slates. Volcanic rocks in the arc are known as Chalt and Shamaran Volcanics, while plutonic rocks are the rocks of Kohistan Batholith and Chilas Complex. Whereas Gilgit Metamorphic Complex contains metasediments with intrusion of Kohistan Batholith. Karakoram Block is part of Eurasian Plate and Karakoram Metamorphic Complex is the southernmost part of the Karakoram Block making boundary with KIA (Petterson and Treloar et al., 2004).

Sharote Valley is located in the northernmost section of the Kohistan Island arc, close to south of the northern suture zone or Main Karakoram Thrust, a tectonic zone that separates the KIA rocks from those of the Karakoram Plate (Fig. 1). Geologically the study area is complex due to its regional scale tectonic involvement. The research area and its surroundings are primarily composed of meta-sediments and Chalt Volcanic Group (CVG) rocks intruded by Kohistan batholith (Petterson, 2010).

Hayden (1914) first reported volcanic rocks at Chitral and Gilgit. Ivanac et al. (1956) later dubbed these rocks as the part of the greenstone complex. With the involvement of regional tectonics, these rocks have undergone varied degrees of metamorphism. Quartzites, hornblende schist, mica schist, hornblende gneiss, marble, limestone, andesite, basalt and rhyolite are some of the rock types found in this complex (Tahirkheli, 1979).

Tahirkheli (1982) measured the greatest thickness of these volcanics in Hunza valley, and they are known as the Rakaposhi volcanic group. Based on their ages, the volcanic sequences are split into two groups. Chalt Volcanic Group is an older group that is more deformed and metamorphosed which are classified by Petterson and Windley (1991) as 1) Hunza volcanics, in the Hunza Valley, and 2), western volcanics, which are found in the western section of Gilgit. Petterson and Treloar (2004) later termed the Hunza volcanics as the Hunza Formation, whereas the western volcanics were termed as Ghizer Formation.

The Ghizer Formation has been further subdivided into three categories. Ishkoman Volcanic Centre (IVC), BASD (dominant by basalt-andesite sheet), and tuff dominating (TD). Pudsey et al. (1985) termed the less deformed/undeformed younger volcanic rocks as Shamran volcanics which are mostly lava flows of basalt-rhyolite, belonging to Paleocene period (Sullivan et al., 1993; Treloar et al., 1996).

Danishwar et al. (2001) termed these volcanics the Teru Volcanic Formation. On the basis of petrographic and geochemical similarities, Sullivan et al. (1993) connected the Shamaran

volcanics with the Western volcanics of Petterson and Windley (1991). Sharote Valley polymetallic deposit is formed of multiple veins, cutting across the plutonic rocks. A rich mineralized vein (Fig. 2) with visible oxides, sulphides and carbonates extending horizontally in north-south direction showing contact with granodiorite of the Kohistan Batholith.

The deposit is formed of sulphide veins and is mainly exposed in contact with metasedimentary (upper contact) and metavolcanic rocks (lower contact). A rich mineralized vein with visible oxide and sulphides contents extending horizontally in north-south direction showing contact with granodiorite of the Kohistan Batholith. Petrographic investigations of the rock show that the major minerals are quartz, biotite, muscovite, epidote, plagioclase and hornblend. with accessory minerals chlorite, sericite, opaques. The ore minerals are mainly bornite, pyrite, galena and azurite.

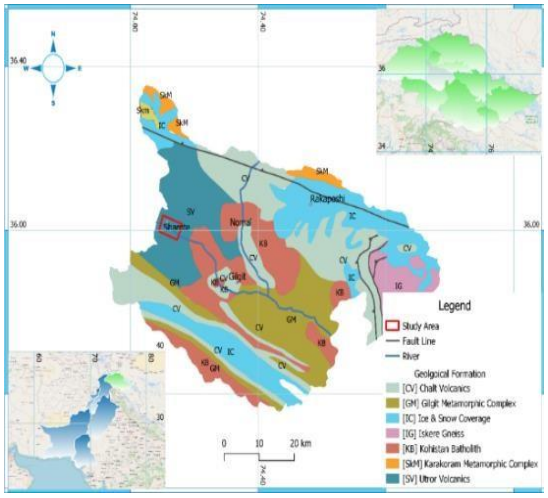

Fig. 1 Geological map of Kohistan terrane, North Pakistan (after Treloar et al., 1996).

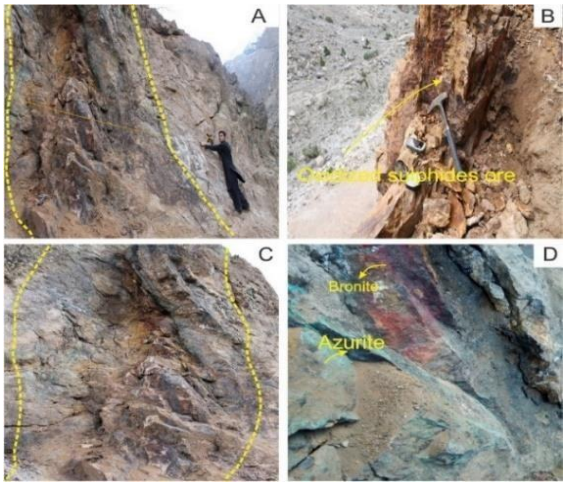

Fig. 2 Ploymetallic veins showing minralizaiton in Sharote polymetallic deposit.

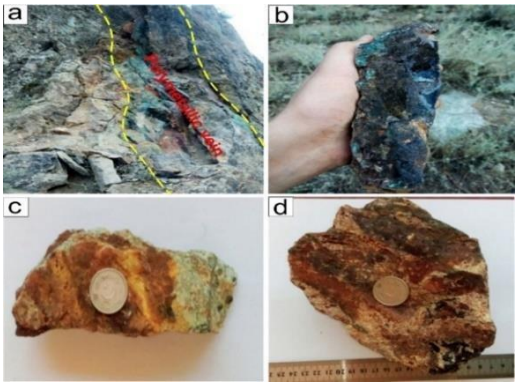

Fig. 3 Shows ore samples.

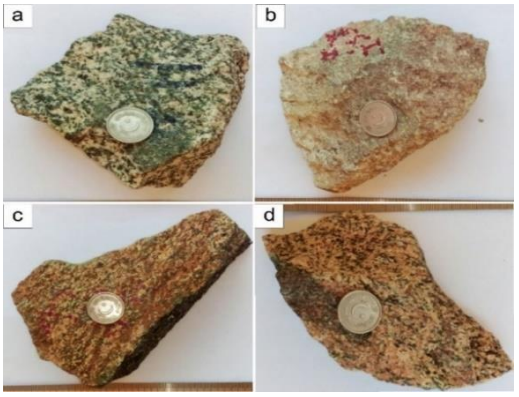

Fig. 4 Shows rock samples from Sharote polymetallic deposit.

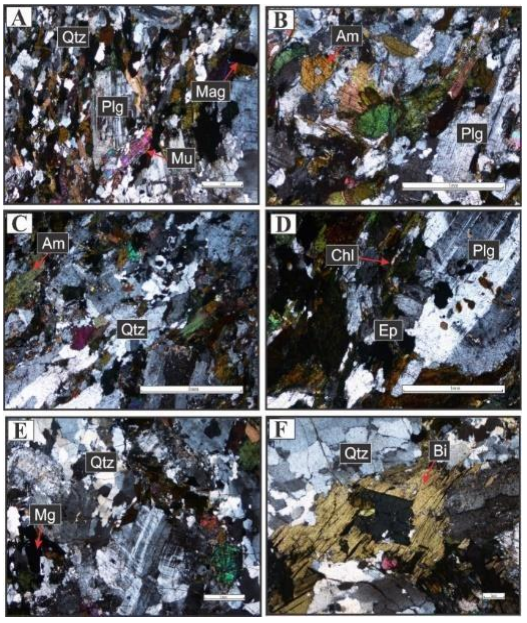

Fig. 5: Photomicrographs (A, B, C, D, E, F: XPL; cross polars) of the samples collected from the associated rock (quartz monzonite) of the sulphide bearing zones. Qtz: quartz, Bi: biotite, Plg: plagioclase, Ep: epidote, Mg: magnetite, Mu: muscovite, Chl: chlorite, am: amphibole (hornblende).

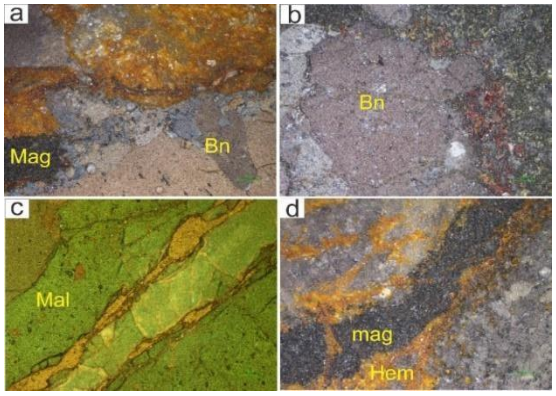

Fig. 6 Photomicrograps of ore, Bn. Bornite, Mag. Magnitite, Hem. Hematite, Mal. Malachite.

Materials and Methods

Sampling

During the fieldwork 20 ore samples and 10 rock samples were collected from the vein as well as associated/host rock. Locations of these samples are shown in Figure 2. Out of these, representative 12 ore and 4 rock samples were selected for different types of analysis and shifted to the National Center of Excellence Geology (NCEG) University of Peshawar to conduct petrographic and geochemical studies.

Analytical Technique

X-ray Fluorescence Spectroscopy: A total of 4 representative associated rock samples from the host rock were analyzed using XRF. These analyses were done for the major elements of the rocks. Whole-rock major elements geochemical analyses of the rock samples were carried out using an energy-dispersive X-ray fluorescence spectrometer (EDX-7000, Shimadzu). Fresh and unaltered rock samples were first cleaned, dried, and crushed using a steel jaw crusher, followed by pulverization in an agate mill to obtain a fine powder (<75 μm) in order to avoid contamination. The powdered samples were then pressed into pellets using a hydraulic press with a suitable binder. The EDX-7000 instrument was operated under standard analytical conditions with appropriate voltage and current settings for major elements.

Calibration was performed using certified reference materials of igneous rocks, and analytical accuracy was monitored through repeated measurements of standards and blanks. Major oxides were reported in weight percent (wt.%), while trace elements were expressed in parts per million (ppm). Analytical precision for major elements was better than ±2%, and for trace elements better than ±5%.

Atomic absorption Spectroscopy: Polymetallic ore samples were analyzed for trace and minor elements using a PerkinElmer Graphite Furnace Atomic Absorption Spectrometer (GF-AAS). Fresh and representative ore samples were carefully cleaned, dried, and crushed, followed by pulverization in an agate mill to obtain a homogeneous powder (<75 μm) and to minimize contamination.

Approximately 0.1 g of powdered sample was digested in Teflon vessels using a mixed-acid digestion procedure (HF–HNO_3–$HClO_4$) to ensure complete dissolution of sulphide and silicate phases. After digestion, the solutions were evaporated to near dryness, treated with dilute HNO_3 to decompose fluoride complexes, and diluted to a known volume with ultrapure deionized water. Elemental concentrations, including Cu, Cr, Zn, Co, Pb, Fe, Mn, Ni, Au,, were determined using graphite furnace AAS under optimized furnace temperature programs for drying, pyrolysis, and atomization.

Calibration was performed using multi-element standard solutions prepared in the same acid matrix as the samples. Analytical accuracy and precision were assessed through repeated analyses of certified reference materials, procedural blanks, and duplicate samples. Analytical precision was generally better than ±5%, with detection limits in the sub-ppm range.

Scanning Electron Microscopy: Model: JSMIT-100 was used to make the SEM samples that were studied. A total of two representative ore samples were analyzed through SEM-EDX (JSMIT-100, Scanning Electron Microscope/Secondary Energy Detector). These samples were cut into small chips through the special cut method and then the studied surfaces were smoothened by rubbing them against the porcelain plates with 1000.0 size powder (silicon carbide powder).

Results and Discussion

Petrogensis

Petrographically the rock is identified as quartz monzonite which comprises of quartz, biotite, muscovite, epidote and chlorite. Chlorite and serecite are formed as the altration products of amphibole and plagioclase. Amphibole is primary and chlorite is secondary. Overall, the rocks is deformed under greenschist facie metamorphism. Plagioclase is also altered as a result of metamorphism into serecite, biotite and chlorite. Hornblende is common as seen in thin section study, very mature and clear two sets of cleavages are oberseved and identified. Percentage wise, the plagioclase and felspar are rather abundant minerals. Quartz is the second more abundant mineral.

Average model mineralogical composition of the four samples is given as following. Plagioclase as observed by the microscope is above 40%, epidote is approximately 5%, chlorite is secondary and produced because of alteration counts for 10%, quartz is light grey and counts for 30%, biotite is yellow to brown approximately 10% in amount, and the miscellaneous minerals count for 5%. Amphibole and some pyroxenes are counted approximately 20% in some samples. Muscovite is aproximately 10% (Fig. 7).

The host rock for sulphide mineralization in the veins and ore deposits is classified as quartz monzonite. The rock is packed with felsic veins, intermediate intrusions and outcrop scale fractures. The fractures, shear and other mechanical discontinuities are common on the outcrop (Fig. 7) Ore bearing zone contains iron, nickel, cobolt, zinc, manganese, gold, chromium, lead, silver and copper. The deposit is formed as a result of hydrothermal process.

Geochemical Characteristics of Ore and Associated Rocks

Major elements: The oxides of major elements encountered in the Sharote valley Polymetallic deposit are shown in Table 2. The major oxides wt. % recorded in the study area are: Na_2O (6.10-6.70 wt. %), CaO (2.73-5.49 wt. %), SiO_2 (66.69-68.10 wt. %), Fe_2O_3 (1.0-3.92 wt. %), showing less variations, while the other major oxides show some variation, like; Al_2O_3 (4.55-8.59 wt. %), and K_2O (2.1-2.28 wt. %). The major oxides in the study area plotted against SiO_2 and Na_2+K_2O (Total Alkalis) and show that the rocks lie in quartz monzonite fields in classification diagram (Middlemost, 1985) for plutonic rocks (Fig. 8).

To observe the variation trend during differentiation of the major oxides, the plots of the Harker diagram are used (Fig. 9). These plots show that the lines of CaO and Na_2O against SiO_2 are smooth and show negative trend, while the K_2O have poorly defined negative trend. Fe_2O_3 and MgO show a weak positive trend against SiO_2.

The poorly defined negative trend shows the secondary alteration (post magmatic activity). These types of variation can be observed in the Calc-alkaline lithologies. To differentiate Calc-alkaline from the Tholeiitic rocks the percentages of these different oxides were then plotted on the AFM ternary diagram of Irvine and Baragar (1971) (Fig. 10), which shows the study area have more Calc-alkaline and less tholeiitic in nature.

Trace elements: Trace elements geochemistry of the ore is predominantly fruitful in terms of precious and base metals mineralization. Certainly, few locations were identified during the field which show potential of ore mineralization in Sharote valley (Table 1).

The deposit have Cu-mineralization in form of malachite (having green color in hand specimen), azurite (blue color in hand specimen) and chalcopyrite, which occurs as several concentrated zones within the host rock. The atomic absorption analysis reveals that copper also is associated with iron, silver, gold and lead. The ore samples (SH1, SH4, SH6, and SH10 show relatively high concentration of copper as 1.3775 wt. %, 1.55125 wt. %, wt. % and 1.4925 wt. % respectively. Cu shows positive trends with Co, Cr, Zn, Ag and Pb.

The trace element compositions of the ore samples are given in Table 2. The analysis shows that elements like Pb (2.1-952 ppm), Si (11188-17575 ppm), Mn (84.7-5490 ppm), and Au (0.032-1.69 ppm), Pb (2.1-952 ppm), Cr (2.25-12.9 ppm), Ag (4.2-43.55 ppm) and Co (78.75-252.5 ppm) display a variable concentration. Fe, Cu, Ni, Co, Zn, Al, Si, and Mg are recorded for MRFE field (Mantle Rock Forming Elements).

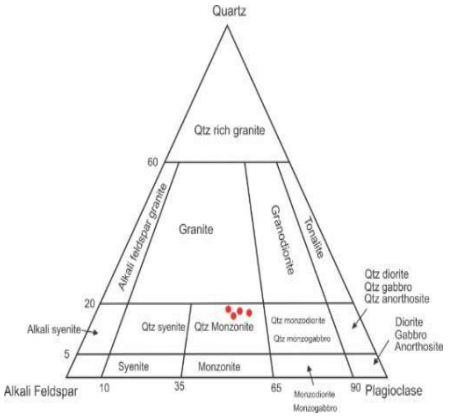

Fig. 7 Plotting of the studied samples of the host rock in IUGS classification of igneous rocks chart. The sample lies in the field of quartz monzonite

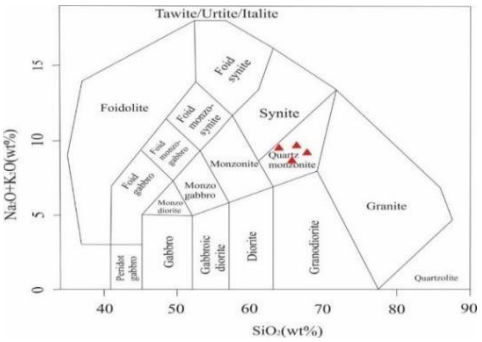

Fig. 8 TAS diagram for the igneous rocks classification (Middlemost, 1985).

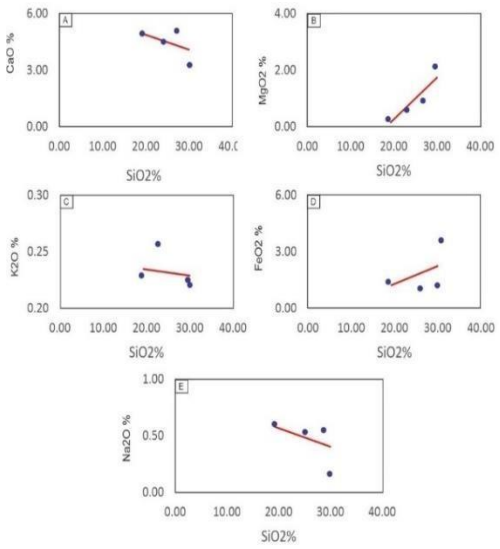

Fig. 9 Major oxide versus silica, Harker diagrams for the host rock.

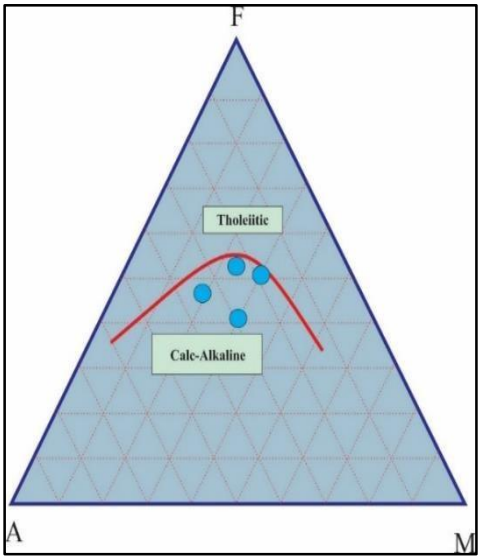

Fig. 10 AFM ternary diagram Plots for the study area, where A (Na_2O+K_2O); F (FeO); M (MgO) (from Irvine and Baragar, 1971).

Table 1. Major elements data of associated rock samples.

S.No	Fe_2O_3%	Na_2O%	K_2O%	Al_2O_3%	SiO_2%	CaO%	MgO%
HR1	3.92	6.2	2.1	8.08	66.69	5.49	2.34
HR2	1.49	6.10	2.8	4.55	67.15	4.88	0.21
HR3	1.10	6.7	2.21	8.59	68.1	2.73	1.27
HR4	1.00	6.30	2.28	4.84	67	4.43	0.86

Table 2. Geochemical data (ppm) of ore samples.

S.No	**Fe%**	**Cu%**	**Cr ppm**	**Pb**	**Ni**	**Co**	**Au**	**Zn**	**Ag**	**Mn**
SH-1	17.325	1.3775	9.05	67.2	28.25	146.25	0.296	235	16.3	1881
SH-2	1.305	0.09788	5.95	2.1	24.5	168.75	0.032	26.7	6.2	410.55
SH-3	14.305	0.54675	8.4	101.15	2.7	220	0.092	70.25	7	2224.5
SH-4	20.943	1.55125	3.15	255	11.85	207.5	0.252	280.45	30.4	5385
SH-5	3.535	0.08513	4.3	907	0.1	131.25	1.69	19.15	43.55	84.7
SH-6	48.413	2.0025	2.25	952	16.25	245	0.204	211.75	41	5490
SH-9	5.2175	0.13025	8.35	11.8	17.25	81.25	0.058	17.45	4.5	130.25
SH-10	36.713	1.4925	4.9	414.85	23.5	252.5	0.38	113.3	14.95	5140
SH-11	16.085	0.68613	5.65	1105	3.4	78.75	0.07	95.05	17.5	4751.5
SH-12	6.76	0.11388	12.9	3.95	2.9	181.25	0.04	29.95	4.2	348.35

SEM-EDX Analysis of Ore Samples

For the SEM-EDX analysis two ore samples containing dominant Cu and Fe were selected for the investigation. The samples were analyzed through line analysis, whole field spectrum, and point composition.

Cu-Ore sample: For the Cu-ore analysis, HR-4 sample was selected for to carry out SEM. For point analysis Energy Dispersive X-ray (EDX) mode was used which gave the chemistry of that selected point in the sample. Based on different brightness variation of the selected sample, different points are noted for SEM analysis. Bright, Light and Dark colors are the different selected points. The lighter color shows the heavier elements and dark coloration shows less density elements. Figure 11 A and B, show the point analysis and the percentages of different minerals are recorded in Table 4.

Point analysis, line analysis and field view analysis for the SEM-EDX, recorded that Cu (Copper) is related with lead (Pb), silicon (Si), oxygen (O), iron (Fe), and aluminum (Al). The relative abundance of elements suggest that copper ore occurs in form of malachite (Cu_2CO_3 (OH) $_2$), azurite ($C_2H_2Cu_3O_8$) and chrysocolla ($Cu_2H_2Si_2O_5(OH)_4$). The average concentration of copper in SEM-EDX point analysis is 0.06-0.14 wt. % and for SEM-EDX analysis. Whereas the Cu concentration determined by Atomic Absorption Spectrophotometer for same sample is 1.37 wt. % (Table 4).

Iron Ore sample: HR-9 was taken as a representative Fe ore sample to examine through SEM. For point analysis Energy Dispersive X-ray (EDX) mode was used which gave the chemical composition of the selected point. Based on different brightness variations of the selected samples, different points are noted for SEM analysis. Bright, Light and Dark colors are the different selected points. The lighter color shows the heavier elements and dark coloration shows less density elements. Figure 12 A and B show the point analysis, and the percentages of different minerals are recorded in Table 5.

Point analysis and field view analysis for the SEM-EDX mode show that iron (Fe) is associated with lead (Pb), oxygen (O), silicon (Si), aluminum (Al) and cobalt (Co). The average concentration of iron in SEM-EDX point analysis is 0.08-2.12 wt. %, whereas the Fe concentration determined by Atomic Absorption Spectrophotometer for same sample is 1.3-2.20 wt. % Table 5.

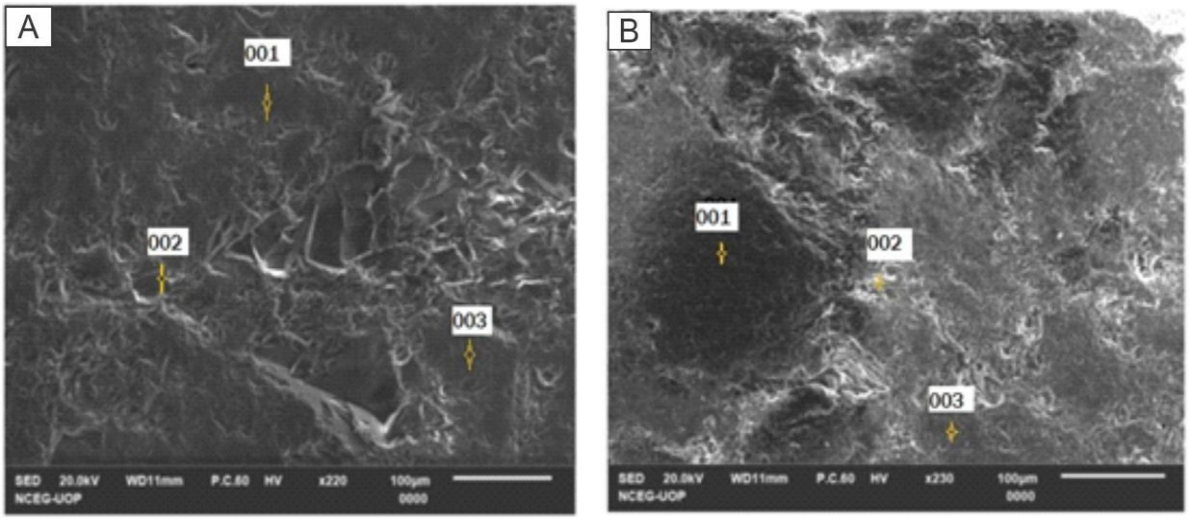

Fig. 11 Images A and B show SEM-EDX point analysis of Cu ore sample HR-04.

Table 3. Elemental composition of Cu ore sample HR-04 (3 points selected with light, light dark, and dark color).

S. No	Si	K	Na	Pb	Mg	O	Al	Fe	Cu
Point 1	26.77	1.03	1.10	0.06	1.48	54.36	9.13	5.83	0.10
Point 2	28.03	1.9	1.22	0.04	1.56	51.02	9.83	6.1	0.17
Point 3	25.03	2.1	1.90	0.86	2.02	50.08	10.02	8.02	1.3

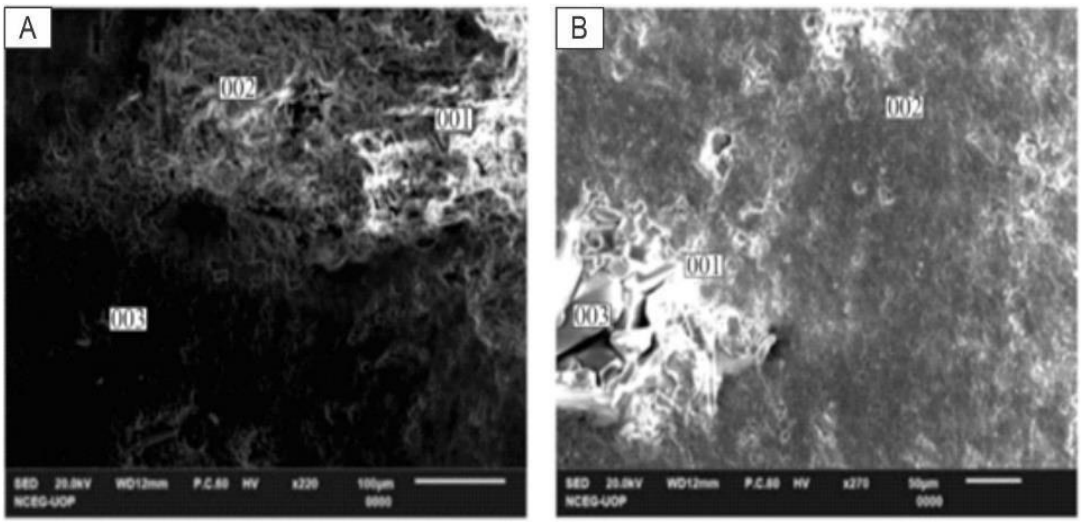

Fig. 12 Images A and B show SEM-EDX point analysis of Fe ore sample HR-09.

Table 4. Elemental composition of Fe ore sample HR-09 (3 points selected with light, light dark, and dark color).

S. No	Si	K	Na	Pb	Mg	O	Al	Fe	Cu
Point 1	18.79	00	00	0.01	1.1	61.36	8.19	2.20	0.0
Point 2	25.56	0.4	0.84	0.04	1.17	53.02	1.70	1.90	0.01
Point 3	21.90	0.1	053	0.09	1.19	49.07	0.05	1.30	0.03

Table 5. Statistical parameters of selective trace elements (ppm) in Sharote study area.

S.No	AU	Ag	Cu	Cr	Pb	Ni	Co	Zn
SH-1	0.296	16.3	13775	9.05	67.2	28.25	146.25	235
SH-2	0.032	6.2	978.75	5.95	2.1	24.5	168.75	26.7
SH-3	0.092	7	5467.5	8.4	101.15	2.7	220	70.25
SH-4	0.252	30.4	15512.5	3.15	255	11.85	207.5	280.45
SH-5	1.69	43.55	851.25	4.3	907	0.1	131.25	19.15
SH-6	0.204	41	20025	2.25	952	16.25	245	211.75
SH-9	0.058	4.5	1302.5	8.35	11.8	17.25	81.25	17.45
SH-10	0.38	14.95	14925	4.9	414.85	23.5	252.5	113.3
SH-11	0.07	17.5	6861.25	5.65	1105	3.4	78.75	95.05
SH-12	0.04	4.2	1138.75	12.9	3.95	2.9	181.25	29.95
Mean	0.3114	18.56	8083.75	6.49	382.005	13.07	171.25	109.91
Median	0.148	15.63	6164.37	5.8	178.075	14.05	175	82.65
Slandered Deviation	0.499	14.82	7320.59	3.201	440.042	10.390	62.11	98.33
Minimum	0.04	4.2	851.25	2.25	2.1	0.1	78.75	17.45
Maximum	0.296	43.55	20025	12.9	1105	28.25	252.5	280.45

Magma Evolution

For the identification of magma generation and tectonic setting, different ternary diagrams are used for the Sharote polymetallic deposit. The most important in these are AFM ternary diagram which is used to differentiate calc-alkaline from the tholeiitic rocks. The percentages of these different oxides were then plotted on the AFM ternary diagram of Irvine and Baragar (1971), which shows the associated rocks are more calc-alkaline and less tholeiitic in nature.

The three corners has three compositions like A (total Alkalis=Na_2O+K_2O); F (Total Iron oxide=FeO); M (Total magnesium oxide=MgO)

(Irvine and Baragar, 1971). From all these analyses the nature of magma was mostly calc-alkaline, which showed a subduction type island arc setting, and the most favorable rock type are plutonic in nature.

Genesis of the Deposit: Sulphide veins containing chalcopyrite and bornite, with secondary azurite and malachite, hosted in quartz monzogranite are best explained by a magmatic–hydrothermal origin related to the emplacement and crystallization of the granitic intrusion. During magma evolution, Cu, Au, Pb, and Fe, together with volatiles (H_2O, S, Cl, CO_2), became concentrated in the residual melt. Once fluid saturation was reached, metal-bearing hydrothermal fluids were exsolved from the crystallizing quartz monzogranite. These fluids were enriched in Cu–Au complexes and represent the primary source of the sulphide mineralization.

As the intrusion cooled, tectonic stresses and thermal contraction generated fractures and vein pathways within the granite. The magmatic fluids migrated through these structures and underwent

changes in temperature, pressure, and chemistry, as well as interaction with the host rock and possible mixing with meteoric fluids. These processes destabilized metal complexes, leading to the precipitation of quartz with chalcopyrite and bornite as the dominant sulphide phases, accompanied by Au and minor Pb-bearing minerals. This mineral assemblage and vein-style geometry are characteristic of granite-related hydrothermal Cu–Au vein systems and may represent a late-stage or distal expression of a porphyry-type system.

Following uplift and exposure, near-surface weathering caused oxidation of the primary copper sulphides. Chalcopyrite and bornite were altered to secondary copper carbonates, forming azurite and malachite in the upper parts of the veins. This supergene overprint indicates post-mineralization oxidation and enrichment processes, while preserving the original magmatic–hydrothermal signature of the sulphide veins at depth**.**

Conclusion

It is concluded that the hydrothermal deposit containing different sulphides was formed in quartz monzonites. Host rocks are altered due to metasomatism and hydrothermal injections that caused the mineralization of the sulphide bearing ores. The most prominent alteration products are chlorite and sericite. These two strikingly demarcate the greenschist facie of metamorphism, under low to high pressure and temperature. The regional geological setup is very active tectonically and several regional faults, shear zones and boundaries crosscut the area. Due to these active zones, the area has been experienced deformational events.

Petrographically, the plagioclase feldspar is abundant mineral. Quartz is the second most abundant mineral. Average model mineralogical composition of the four samples is given as following. Plagioclase as observed beneath the microscope is above 40%, epidote is approximately 5%, chlorite is secondary and produced because of alteration counts for 10%, quartz is light grey and counts for 30%, biotite is yellow to brown approximately 10% in amount, and the miscellaneous minerals counts for 5%.

Amphibole (and some pyroxene) are counted approximately 20% in some samples. Muscovite is approximately 10%. The host rock for sulphides mineralization in the veins and ore deposits is classified as quartz monzonite. The rock is packed with felsic veins, intermediate intrusions and outcrop scale fractures. Fractures, shear ‘and other mechanical discontinuities are common on the outcrop. Ore bearing zone contains iron, nickel, cobalt, zinc, manganese, gold, chromium, lead, silver and copper. The deposit is formed due to hydrothermal processes.

Based on geochemistry, the analyzed samples contain Au from 0.032-0.296 ppm with an average of 0.3114 ppm, and Ag from 4.2-43.55 ppm (18.56 ppm average). The content of Cu ranges from 851.25-20025 ppm with a mean value of 8083.75 ppm. While Cr contents range from 2.25-12.9 ppm with a mean of 6.49 ppm. The contents of Pb, Ni and Co range from 2.1-1105 ppm, 28.25ppm and 78.75-252.5 ppm with a mean concentration of 382.005 ppm, 13.07 ppm and 171.25 ppm, respectively.

While Zn contents were measured from 17.45-280.45 ppm with an average of 109.905 ppm. Based on the present investigation (Geochemical analysis and petrographic), it is suggested that the area have economic minerals concentrations which can be further explored through geophysical techniques.

Acknowledgement

We are highly thankful to Professor Qasim Jan for his valuable help in petrography. This study is funded by ORIC Karakoram International University, grant No: KIU-ORIC-1(2021/025.

References

Bauer, P., Palm, S., Handy, M. R., (2000). Strain localization and fluid pathways in mylonite:

inferences from in situ deformation of a water-bearing quartz analogue (norcamphor). *Tectonophysics*, **320**(2), 141-165.

Brill, B. A. (1989). Trace-element contents and partitioning of elements in ore minerals from the CSA Cu-Pb-Zn deposit, Australia, and implications for ore genesis. *The Canadian Mineralogist*, **27**(2), 263-274.

Burg, J. P., Bodinier, J. L., Chaudhry, S., Hussain, S., Dawood, H. (1998). Infra-arc mantle-crust transition and intra-arc mantle diapirs in the Kohistan Complex (Pakistani Himalaya): Petro-structural evidence. Terra Nova-Oxford, **10**(2), 74-80.

Calkins, J. A., Jamiluddin, S., Kamaluddin, B., Hussain, A. (1969). Geology and mineral resources of Chitral state, West Pakistan. Geological Survey of Pakistan, Unpublished report- Quetta.

Danishwar, S., Stern, R. J., Khan, M. A. (2001). Field relations and structural constraints for the Teru volcanic formation, Northern Kohistan Terrane, Pakistani Himalayas. *Journal of Asian Earth Sciences*, **19**, 683-695.

Evans, A. M. (2009). Ore geology and industrial minerals: An introduction, John Wiley & Sons.

Hayden, H. H. (1914). Notes on the geology of Chitral and Gilgit and the Pamirs. Records of the Geological survey of India, **45,** 271-335.

Irvine, T. N., Barager, W. R. A. (1971). A guide to the chemical classification of the common volcanic rocks. *Canadian Journal of Science*, **8**, 523-548.

Ivanac, J. F., Traves, D. M., King, D. (1956). The geology of the northwest portion of Gilgitagency. Records of Geological Survey of Pakistan, **8** (2), 3-26.

Kiptarus, J. J., Muumbo, A. M., Makokha, Makokha, A. B., Kimutai, S. K. (2015). Characterization of selected mineral ores in the eastern zone of Kenya: Case study of Mwingi North Constituency in Kitui County. *International Journal of Mining Engineering and Mineral Processing*, **4**(1), 8-17.

Kyser, T. K. (2007). Fluids, basin analysis, and mineral deposits. *Geofluids*, **7**(2), 238-257.

Middlemost, E. A. K. (1985). Magmas and magmatic rocks: An introduction to igneous petrology, 1–266. Longman: London and UK.

Niu, S. D., Li, S. R., Santosh, M., Zhang, D. H., Li, Z. D., Shan, M. J., Zhao, W. B. (2016). Mineralogical and isotopic studies of base metal sulfides from the Jiawula Ag–Pb–Zn deposit, Inner Mongolia, NE China. *Journal of Asian Earth Sciences*, **115,** 480-491.

Pearce, J. A., Cann, J. R. (1973). Tectonic setting of basic volcanic rocks determined using trace element analyses. *Earth and Planetary Science Letters*, **19**, 290-300.

Petterson, M. G., Treloar, P. J. (2004). Volcano-stratigraphy of arc volcanic sequences in the Kohistan arc, North Pakistan: volcanism within island arc, back-arc-basin, and intra-continental tectonic settings, *Journal of Volcanology and Geothermal Research*, **130,** 147-178

Petterson, M. G., Windley, B. F. (1991). Changing source regions of magmas and crustal growth in the Trans-Himalayas: Evidence from the Chalt volcanics and Kohistan batholith, Kohistan. 326-341

Pudsey, C. J., Schroider, R., Skelton, P. W. (1985). Cretaceous (Aptian/Albian) age for island arc volcanics. Kohistan, N. Pakistan. Contribution to the *Himalayan Geology*, **3**, 150-168.

Robb, L. (2005). Introduction to Ore-Forming Processes. Black Publisher, Australia.

Saunders, A. D., Tarney, J. (1991). Back-arc basins. In: Floyd, P. A. (eds.) Oceanic basalts. Blackie and Nostrand Teihold, 219-263.

Shervais, J. W. (1982). Ti-V plots and the petrogenesis of modern and ophiolitic lavas. *Earth and Planetary Science Letters*, **59**, 101-118.

Smith, R. E., Smith, S. E. (1976). Comments on the use of Ti, Zr, Y, Sr, K, P, and Nb in classification of basaltic magmas. *Earth and Planetary Science Letters*, **32**, 114-120.

Sullivan, M. A., Windley, B. F., Saunders, A. D., Haynes, J. R., Rex, D. C. (1993). A palaeogeographic reconstruction of the Dir Group: Evidence for magmatic arc migration within Kohistan, N, Pakistan. *Geological Society Special Publication*, **74**, 139-160.

Tahirkheli, R. A. K. (1979a). Geology of Kohistan and adjoining Eurasian and Indo-Pakistan continents, *Pakistan. Geol. Bull., Univ. Peshawar*, **11**, 1-30.

Tahirkheli, R. A. K. 1982. Geology of the Himalaya, Karakoram and Hindukash in *Paksitan. Geological Bulletin, University of Peshawar*, 15, 1-50.

Tahirkheli, R. A. K., Jan, M. Q. (1979). Preliminary geological map of Kohistan and adjoining areas, Geol. of Kohistan Northern Pakistan, *Geol. Bull. Univ. Peshawar*, (Spec. Issue), **11**.

Treloar, P. J., Petterson, M. G., Jan, M. Q., Sullivan, M. A. (1996). A re-evaluation of the stratigraphy and evolution of the Kohistan arc sequence, Pakistan Himalaya: Implications for magmatic and tectonic arc-building processes. *Journal of the Geological Society, London*, **153**, 681-693

Wilson, M. (1989). Igneous petrogenesis. Unwin Hyman, London.

Wood, D. A., Joron, J. L., Treuil, M. (1979). A re-appraisal of the use of trace elements to classify and discriminate between magma series erupted in different tectonic settings. *Earth and Planetary Science Letters,* **45** 326-336.